

# Structural manipulation of $\text{YBa}_2\text{Cu}_3\text{O}_{7-\delta}$ (YBCO) superconductors *via* melt-textured growth with $\text{BaTiO}_3$ epitaxial seed

M. S. A. Jawari<sup>1</sup>, S. K. Chen<sup>2</sup>, S. A. Halim<sup>2</sup>, Z. A. Talib<sup>2</sup> and O. J. Lee<sup>3\*</sup>

<sup>1</sup>*School of Ocean Engineering, Universiti Malaysia Terengganu, 21030 Kuala Terengganu, Terengganu*

<sup>2</sup>*Department of Physics, Faculty of Science,*

*Universiti Putra Malaysia, 43400 Serdang, Selangor.*

<sup>3</sup>*Advanced Nano Materials (ANoMa) Research Group, School of Fundamental Science,*

*Universiti Malaysia Terengganu, 21030 Kuala Nerus, Terengganu.*

Exploiting the merits of superconducting properties, a series of thermal profile was employed to modify the melt-textured growth of Y–Ba–CuO bulk with  $\text{BaTiO}_3$  epitaxial crystal seed. Two thermal routes were used whereby multiple heatings of the samples were conducted at 940 °C and 960 °C before elevating to 1040 °C and 1070 °C, respectively. Our finding shows that the optimum melt-textured growth window is narrow within the temperature range of 1010–1040 °C. Above the peritectic temperature, partial decomposition of  $\text{YBa}_2\text{Cu}_3\text{O}_{7-\delta}$  (Y123) into  $\text{YBa}_2\text{Cu}_3\text{O}_5$  (Y211) leads to the formation of Y211 multigrains embedded in the matrix of Y123. The values of  $T_c$  for the superconducting Y123 obtained using the two routes are 78 K and 71 K. The lower  $T_c$  suggests the presence of structural distortion and non-stoichiometry of the samples.

**Keywords:** YBCO, melt-textured growth, Y211 facets,  $\text{BaTiO}_3$  epitaxial seed

## I. INTRODUCTION

For decades, single grain RE-BaCuO (RE-rare earth such as Y, Gd and Sm, Nd etc) superconductors have been researched intensively owing to their significant ability to stabilise and trap magnetic field that greater than a permanent magnet [1]. Such a remarkable capability promises a wide variety of applications including magnetic bearing, magnetic separation device and flywheels energy storage [2]. In order to obtain excellent superconducting properties, especially high critical current density and

trapped field, a single grain superconductor is a must. The existence of multigrains and grain boundaries interrupts the flow of supercurrent and thus resulting in low trapped field [3]. There is a close correlation between the properties and the microstructure of the melt-textured bulk superconductors.

Among the fabrication techniques, top seeded melt growth (TSMG) is the well-established method to synthesize single grain superconductors [4]. It has been reported that the  $\text{YBa}_2\text{Cu}_3\text{O}_{7-\delta}$  (Y123) superconductor pellet heated above the peritectic temperature shows

decomposition of  $\text{YBa}_2\text{Cu}_3\text{O}_5$  (Y211) The seed crystal enables preferential heterogeneous nucleation to occur at peritectic solidification of Y123 leading to grain formation with a single crystallographic orientation [5].

Growth temperature window and slow cooling rate are the key parameters which determine the size, morphology and distribution of Y211 inclusions in the Y123 bulk. The inclusion of Y211 phase in the matrix of Y123 bulk is crucial to control the critical current density,  $J_c$  as well as field trapping. One way to tune the Y211 inclusions is to control the infiltration temperature carefully [1]. Secondly, the proportion and particle size of Y211 and Y123 precursor are varied prior to the melt-texture growth [3]. A buffer pellet can be inserted as well to act as a pseudo seeding source and simultaneously prevent contamination on the initial seed [6].

Interestingly, it has been reported that the non-single-grain YBCO and GdBCO-Ag bulk superconductors can be recycled and refabricated by reintroducing the liquid phase into melt process without the need to re-grinding into powder [7]. A liquid phase pellet of  $\text{Y}_2\text{O}_3$ :  $\text{CuO}$ :  $\text{BaCuO}_2$  with 1:6:10 molar ratio was used as liquid phase reinforcement.

The ultimate goal of TSMG technique is to investigate a prudent way to fine-tune the Y211 inclusions in the final Y123 bulk for functionality enhancement. In this work, we have taken up the task of growing Y-Ba-Cu-O (YBCO) superconductor bulk with an unconventional crystal seed.

The  $\text{BaTiO}_3$  epitaxial film is used as crystal seed instead of YBCO single crystal.  $\text{BaTiO}_3$  possesses low lattice mismatch with Y123 with  $a$ ,  $b$  and  $c$  lattice parameters of 0.3962 nm. These lattice parameters are very close and compatible to the lattice parameters of YBCO of  $a = 0.3822\text{nm}$ ,  $b = 0.3888\text{nm}$  and  $c = 1.1701\text{nm}$ .

## II. MATERIALS AND METHODS

Solid state reaction method was employed to produce samples of Y123. The starting raw powders are  $\text{Y}_2\text{O}_3$  (99.9%),  $\text{BaCuO}_3$  (99.8%),  $\text{CuO}$  (99.7%) and  $\text{CaO}$  (99.95%). The raw materials were well mixed according to the nominal stoichiometric ratio. The powders were ground and pressed into circular pellets (about 2 mm thickness and 13 mm diameter) using a hydraulic press with an applied pressure load of 5 tons. Lastly, the pellets were sintered at 920 °C for 15 hours and slowly cooled to 650 °C at the rate of 1°C/ min for 8 hours (annealing process) before further cooling to room temperature. The sintering and annealing process were done under a constant oxygen flow (150 ml/min).

The  $\text{BaTiO}_3$  epitaxial films were grown epitaxially on (100)  $\text{SrTiO}_3$  substrates via pulsed laser deposition. The detailed description of deposition parameters was reported in (Lee *et al.*, 2017) [8]. The epitaxial  $\text{BaTiO}_3$  was placed on the top of each Y123 pellets with the film surface facing down. These sample assemblies were subjected to a series of thermal profiles that in-

cluded initial heating 940 °C and followed by 960 °C before elevating to 1040 °C and 1070 °C for route A and B, respectively. After dwelling for an hour, both samples were rapidly cooled to 1010 °C, then slow cooling at 0.5 °C per hour to 980 °C and lastly, furnace cooling to room temperature. The thermal profiles used for the growth of YBCO samples are shown in Figure 1. Phase formation and crystal structure of the samples were checked by X-ray diffraction (XRD) method using the Rigaku Miniflex II X-ray diffractometer with Cu-K $\alpha$  radiation source. The scanning was carried out in the 2 range of 20° - 80° with the increment step size of 0.02°. Morphology of the grains and the elemental analysis were undertaken using a scanning electron microscope (SEM) model JEOL 6360 LA equipped with energy dispersive X-ray spectrometer (EDX). Superconducting properties of the samples were measured using the standard four-point probe measurement with close-cycle cryostat setup.

### III. RESULTS AND DISCUSSIONS

#### A. Phase formations

Figure 2 shows the XRD patterns of the pure Y123 bulk and BaTiO $_3$  epitaxial film. From Figure 2(a), it is clear that most of the peaks were indexed to Y123 with orthorhombic crystal structure and Pmmm space group (ICSD: 01-078-2144). The peaks with high intensity of

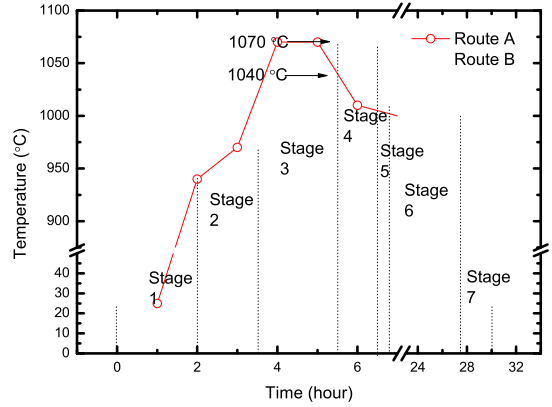


Figure 1. Temperature-time profiles for the growth of YBCO bulks via route A and B

Y123 were observed at  $2\theta \approx 32.9^\circ$  and  $2\theta \approx 33.1^\circ$  that correspond to (103) and (110) reflection. The calculated *a, b, c*-lattice parameter for the orthorhombic Y123 is 0.3822(4) nm, 0.3887(9) nm and 1.1675(0) nm, respectively. The periodical peaks in Figure 2(b) indicate the (00*l*) reflections of BaTiO $_3$  crystal seed grown on (001) SrTiO $_3$  with cubic lattice parameters of  $a = b = c = 0.3962(4)$  nm

#### B. Microstructure manipulations

There is no single grain of Y123 with four-fold growth boundaries fabricated via the route A and B thermal profiles. The growth window of a single grain is narrow and very sensitive to changes in the growth variables and thus leading to the likelihood of multigrains growth. SEM images in Figure 3 indicate that BaTiO $_3$  promotes nucleation and assists the growth of Y211 faceted rods which are observed on the top

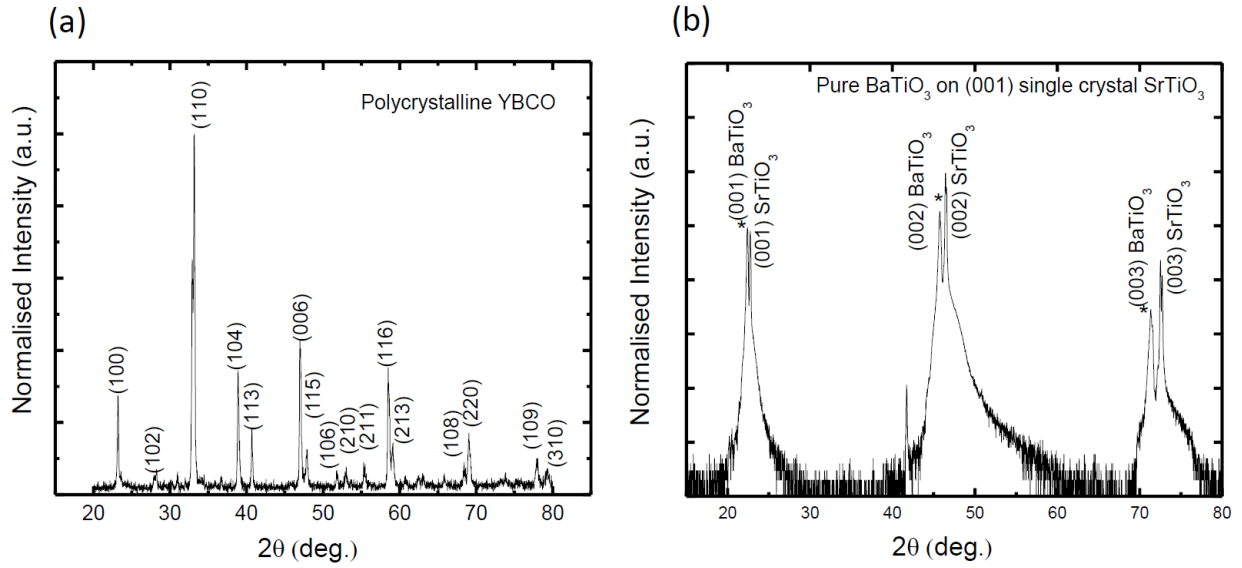


Figure 2. XRD patterns of (a) YBCO bulk (b)  $\text{BaTiO}_3$  seed crystal grown on (001)  $\text{SrTiO}_3$

surface of the  $\text{BaTiO}_3$  seed crystal and melt-textured YBCO pellet. Both samples synthesized via route A and B suffer from incomplete growth with the presence of truncated square and faceted rod of Y211 phase. The incomplete growth produces the superconducting Y123 matrix with discrete and random distribution of non-superconducting Y211 facets. Such faceted inclusions appear in both samples synthesized via route A and B are subjected to elevated temperature above the peritectic reaction of  $1010^\circ\text{C}$  for YBCO system [2].

These results are consistent with the finding by Yang *et al.* (2016) that the single grain of the YBCO bulk is completely destroyed when the heating temperature is greater than  $1020^\circ\text{C}$  [2]. The average facet rod width and length are about  $10.4\ \mu\text{m}$  and  $33.3\ \mu\text{m}$ , respectively. In contrast, there is a minute expansion of ap-

proximately  $2\ \mu\text{m}$  in width and length of Y211 rods fabricated through route B. Hence, the average width and length of these Y211 rods is  $12.3\ \mu\text{m}$  and  $35.6\ \mu\text{m}$ , respectively. The agglomeration effect with smudging rod edges due to higher temperature is noticed as well. According to Namburi *et al.*, 2016, the Y211 non-superconducting phase can act directly as flux pinning centres to improve current density and field trapping in the single grain YBCO superconductor bulks [5]. In addition, the dislocation and stacking faults in the vicinity of the Y211 phase as well as the interface between Y123 matrix and Y211 inclusions may be responsible for flux pinning. However, the flux pinning ability may be vanished if the Y211 pinning centre is much larger (in microns) as compared to the superconducting coherence length (typically tens of nm). As shown in Figure 4, there are cracks

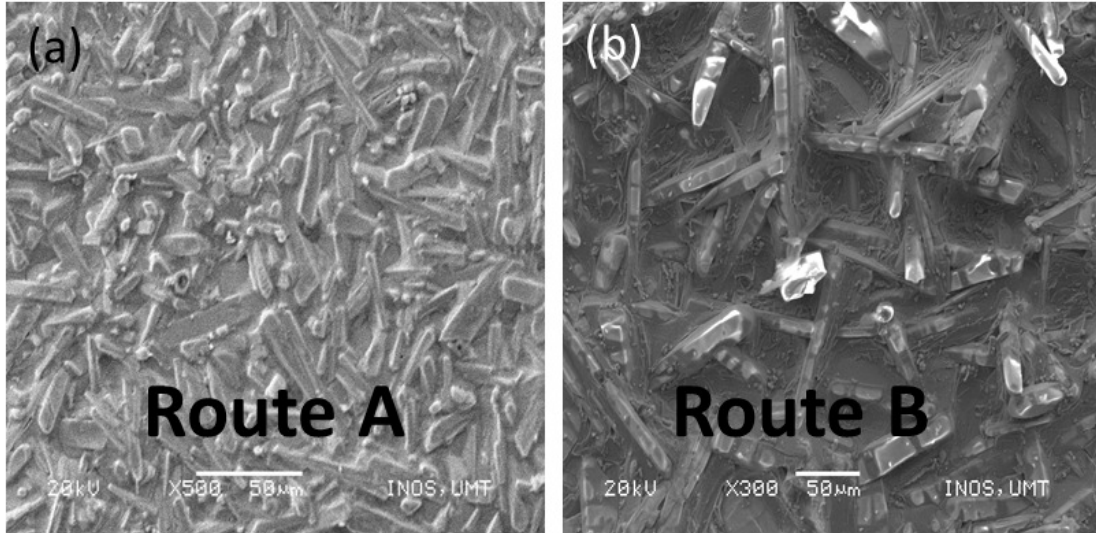


Figure 3. SEM images of melt-textured YBCOs obtained via (a) route A and (b) route B with the distribution of micron-sized Y211 facet rods

around the edge of the crystal seed with a large void (width:  $10\ \mu\text{m}$  and length:  $25\ \mu\text{m}$ ) on the surface of YBCO for route B heating profile due to the out-flowing of Ba-Cu-O melting liquid during the peritectic reaction. It can be seen that the heating performed at lower temperature  $1040\ ^\circ\text{C}$  (as depicted in Figure 3(a)) yields horizontal embedded Y211 facets whereas the tilted and protruded Y211 facets are found on the sample heated at  $1070\ ^\circ\text{C}$ . Given that the melt-textured growth performed at higher temperature results in coarsening of Y211 constituents, temperature range of  $1010 - 1040\ ^\circ\text{C}$  is the optimum heating window.

The critical temperature,  $T_c$  of melt-textured YBCOs was determined from the temperature dependent resistive transition plots. In order to record changes in voltage as the temperature went down, a small current of  $0.03\ \text{A}$  was ap-

plied to the sample.  $T_{c-offset}$  is defined as the superconducting transition temperature for the resistance to drop to zero while  $T_{c-onset}$  is defined as the temperature at which the resistance drops abruptly showing the deviation from linearity of the resistance versus temperature plot. Plots of normalized resistance versus temperature for the melt-textured YBCOs in the range of  $50 - 300\ \text{K}$  are shown in Figure 5. The plots were obtained by normalizing the measured resistance to that at room temperature resistance for each of the sample.  $T_c$  decreases as the melt-textured growth temperature of YBCOs is increased from  $1040\ ^\circ\text{C}$  to  $1070\ ^\circ\text{C}$ . The YBCOs obtained via route A and B show the  $T_c$  of  $78\ \text{K}$  and  $71\ \text{K}$ , respectively and their  $T_{c-offset}$  are  $75\ \text{K}$  and  $66\ \text{K}$ . These values are much lower than that reported for pure YBCO superconductor of  $92\ \text{K}$  suggesting some structural distortion and

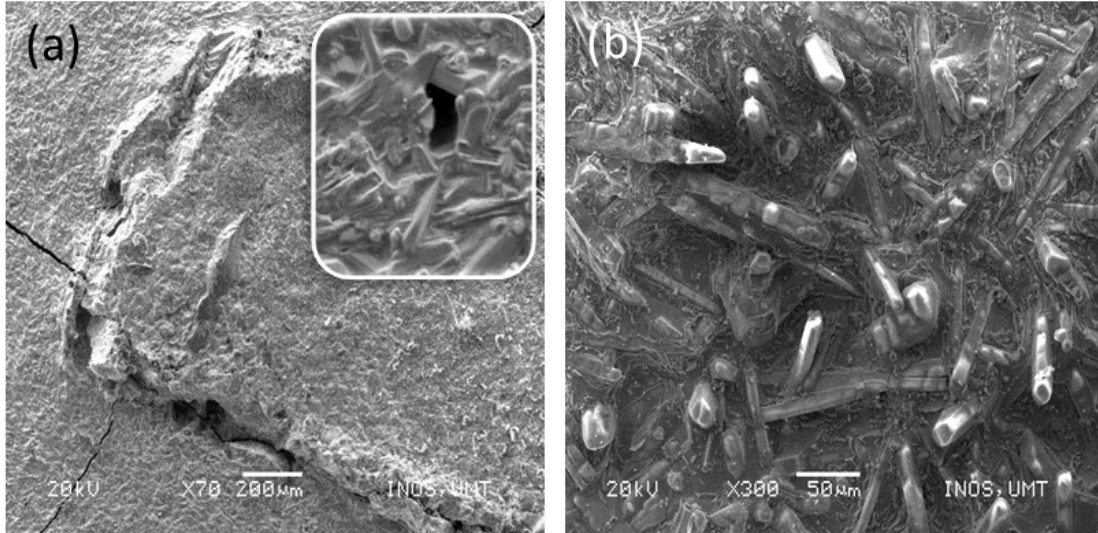


Figure 4. SEM images of the melt-textured YBCO via route B with (a) cracks around the crystal seed and (inset) void as well as (b) protrude micron-sized Y211 facet rods

compositional non-stoichiometry in the samples. The formation of multigrains naturally gives rise to the presence of grain boundaries in the melt-textured YBCO. Consequently, the grain boundaries may act as physical barriers to suppress the super current and therefore limit the field trapping ability of the samples [9].

#### IV. SUMMARY

This study reports melt-textured growth of YBCOs with  $\text{BaTiO}_3$  epitaxial film as crystal seed. According to the observed melting condition, the formation of multigrains occurred whereby the Y211 constituents are embedded in the Y123 matrix. The melt-textured growth window is rather narrow as the optimum heating temperature falls within the temperature range of 1010 - 1040 °C. The lower  $T_c$  for both YB-

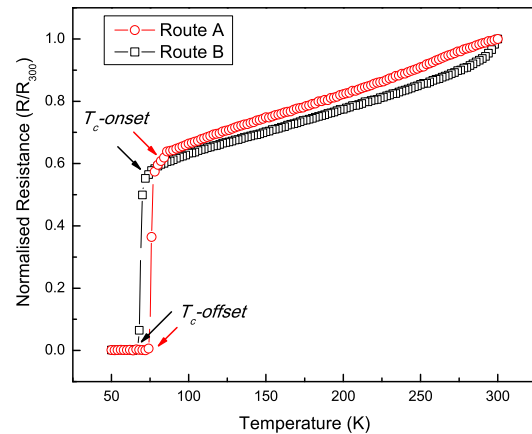


Figure 5. Normalized resistance versus temperature plots for YBCOs obtained via route A and B.

COs obtained via route A and B may be caused by structural distortion and non-stoichiometry of the chemical composition.

- 
- [1] Ouerghi, A, Moutalbi, N, Noudem, J,G, M'chirgui, A, 2017, The Influence of Slow Cooling on Y211 Size and Content in Single-Grain YBCO Bulk Superconductor through the Infiltration-Growth Process, *Physica C*, vol. 534, pp.37-44.
- [2] Yang, C,M, Huang, Y,C, Chen, I,G, Wu, M,K, 2016, Novel LoadingFree Joining Process for YBCO SingleGrain Bulks, *Journal of the American Ceramic Society*, vol. 99(11), pp.3581-3585.
- [3] Thoma, M, Shi, Y, Dennis, T, Durrell, J, Cardwell, D, 2015, Effect of Y-211 Particle Size on the Growth of Single Grain YBaCuO Bulk Superconductors, *Journal of Crystal Growth*, vol. 412, pp.31-39.
- [4] Namburi, D,K, Shi, Y, Palmer, K,G, Dennis, A,R, Durrell, J,H, Cardwell, D,A, 2016, An Improved Top Seeded Infiltration Growth Method for the Fabrication of YBaCuO Bulk Superconductors, *Journal of the European Ceramic Society*, vol. 36(3), pp.615-624.
- [5] Namburi, D,K, Shi, Y, Palmer, K,G, Dennis, A,R, Durrell, J,H, Cardwell, D,A, 2016, A Novel, Two-Step Top Seeded Infiltration and Growth Process for the Fabrication of Single Grain, Bulk (RE) BCO Superconductors, *Superconductor Science and Technology*, vol. 29(9), pp. 095010.
- [6] Shi, Y, Namburi, D,K, Wang, M, Durrell, J, Dennis, A, Cardwell, D, 2015, A Reliable Method for Recycling (RE)BaCuO (RE: Sm, Gd, Y) Bulk Superconductors, *Journal of the American Ceramic Society*, vol. 98(9), pp.2760-2766
- [7] Congreve, J,V, Shi, Y,H, Dennis, A,R, Durrell, J,H, Cardwell, D,A, 2016, Microstructure and Composition of Primary and Recycled Single Grains of YBCO, GdBCOAg, and SmBCOAg Bulk Superconductors, *Journal of the American Ceramic Society*, vol. 99(9), pp. 3111-3119.
- [8] Lee, O, Kursumovic, A, Bi, Z, Tsai, C,F, Wang, H, MacManusDriscoll, J,L, 2017, Giant enhancement of Polarization and Strong Improvement of Retention in Epitaxial Ba<sub>0.6</sub>Sr<sub>0.4</sub>TiO<sub>3</sub>Based Nanocomposites, *Advanced Materials Interfaces*, vol. 4(15), pp.1700336.
- [9] Tang, T,W, Cao, Y, Wu, D,J, Xu, K,X, 2016, A Modified Multi-Seeding Approach for YBCO Bulk Superconductors using Y<sub>2</sub>BaCuO<sub>5</sub> buffer process, *Journal of Alloys and Compounds*, vol. 673, pp.170-174.